Original Research Article

Chemical Reaction and Radiative MHD Heat and Mass Transfer Flow with Temperature Dependent Viscosity past an Isothermal Oscillating Cylinder

ABSTRACT

The numerical analysis is performed to examine the effects of magnetic, radiation and chemical reaction parameters on the unsteady heat and mass transfer flow past a temperature dependent viscosity of an isothermal oscillating cylinder. The dimensionless momentum, energy and concentration equations are solved numerically by using explicit finite difference method. The velocity, temperature and concentration field are analyzed for different well-known parameters. Skin-friction, rate of heat transfer, streamlines and isotherms of different well-known parameters entering into the problem separately are discussed with the help of graphs.

Keywords: Chemical reaction, magnetic, Radiation, Oscillating Cylinder, explicit finite difference.

1. INTRODUCTION

Magneto hydrodynamic, heat and mass transfer flow in an oscillating cylinder has a wide range of applications in the field of geophysical and engineering applications. Now a day MHD flow, heat and mass transfer in a cylindrical bodies have attracted a lot of researchers. Abd EL–Naby *et al.* (2004) presented finite difference solution of radiation effects on MHD unsteady free-convection flow on vertical porous plate. Dufour and soret effects on mixed convection flow past a vertical porous flat plate with variable suction have been studied by Alam *et al*. (2006). Popiel (2008) presented free convection heat transfer from vertical slender cylinder. Numerical study of free convection magneto hydrodynamic heat and mass transfer from a stretching surface to a saturated porous medium with soret and dufour effects is presented by Beg Anwa *et al*. (2009). Mass transfer effects on MHD flow and heat transfer past a vertical porous plate through porous medium under oscillatory suction and heat source studied by Das *et al.* (2009). M. Gnaneswara Reddy(2009) who used Rosseland approximation to describe radiation and mass transfer effects on unsteady MHD free convection flow of an incompressible viscous fluid past a moving vertical cylinder. Rani *et al.* (2010) studied about a numerical study on unsteady natural convection of air with variable viscosity over an isothermal vertical cylinder. An implicit finite Crack-Nicolson method have been used by Gnaneswara Reddy Machireddy(2013) to solve chemically reactive species and radiation effects on MHD convective flow past a moving vertical cylinder. Hossain *et al.* (2015) studied about a numerical study on unsteady natural convection flow with temperature dependent viscosity past an isothermal vertical cylinder. Free convection and mass transfer flow through a porous medium with variable temperature have been presented by Mondal *et al.* (2015). MHD flow, heat and mass transfer due to auxiliary moving cylinder in presence of thermal diffusion, radiation and chemical reactions in a binary fluid mixture have been studied by Sharma *et al.* (2015). Rajesh *et al*. (2016) studied finite difference analysis of unsteady MHD free convective flow over moving semi-infinite vertical cylinder with chemical reaction and temperature oscillation effects.

The principal objective of this research is to investigate the effect of radiation, chemical reaction, heat and mass transfer effect on unsteady MHD free convection flow with temperature dependent viscosity past an isothermal oscillating cylinder. Then these governing equations will be transformed into dimensionless momentum, energy and concentration equations and then the equations will be solved numerically by using explicit finite difference technique with the help of a computer programming language COMPAQ VISUAL FORTRAN 6.6a.

2. MATMEMATICAL MODEL OF THE FLOW

A two-dimensional unsteady free convection flow of a viscous incompressible electrically conducting and radiating optically thick fluid past an impulsively started semi-infinite oscillating cylinder of radius r_0 is considered. Here the x-axis is taken along the axis of cylinder in the vertical direction and the radial coordinate r is taken normal to the cylinder. Initially the cylinder and the fluid are at the same temperature T'_∞ and concentration C'_∞. At time $t' > 0$, the cylinder starts moving in the vertical direction with a uniform velocity u_0.

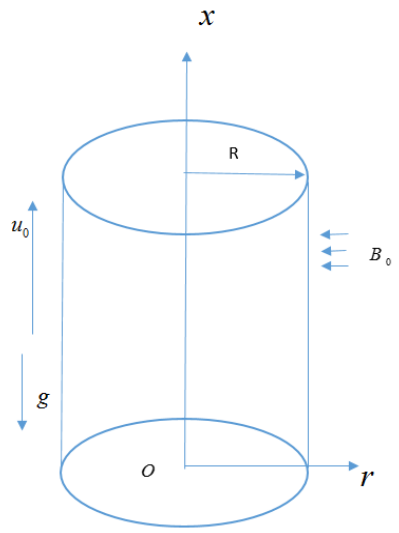

Fig-1: Flow model and Physical Co-ordinate.

The temperature of the surface of the oscillating cylinder is increased to T'_w and concentration C'_w and are maintained constantly thereafter. A uniform magnetic field is applied which is in the direction perpendicular to the oscillating cylinder. The magnetic field is considered to be slightly conducting. It is further assumed that there is no applied voltage, so that electric field is absent. It is also assumed that the irradiative heat flux in the x -direction is negligible as compared to that in the radial direction and the viscous dissipation is also assumed to be negligible in the energy equation due to slow motion of the cylinder. It is also assumed that there exists a homogeneous first order chemical reaction between the fluid and species concentration. But here we assume the level of species concentration to be very low and hence heat generated during chemical reaction can be neglected. In this reaction, the reactive component given off by the surface occurs only in very dilute form. Hence, any convective mass transport to or from the surface due to a net viscous dissipation effects in the energy equation are assumed to be negligible. It is also assumed that all the fluid properties are constant except that of the influence of the density variation with temperature and concentration in the body force term. The foreign mass present in the flow is assumed to be at low level, and Soret and Dufour effects are negligible. Then, the flow under consideration is governed by the following system of equations:

$$\frac{\partial(ru)}{\partial x}+\frac{\partial(rv)}{\partial r}=0 \tag{1}$$

$$\frac{\partial u}{\partial t'}+u\frac{\partial u}{\partial x}+\frac{\partial u}{\partial r}=g\beta\left(T'-T_\infty'\right)+g\beta^*\left(C'-C_\infty'\right)+\frac{1}{r}\frac{\partial}{\partial r}\left(\upsilon r\frac{\partial u}{\partial r}\right)-\frac{\sigma B_0^2}{\rho}u \tag{2}$$

$$\frac{\partial T'}{\partial t'}+u\frac{\partial T'}{\partial x}+\frac{\partial T'}{\partial r}=\frac{\alpha}{r}\frac{\partial}{\partial r}\left(r\frac{\partial T'}{\partial r}\right)-\frac{1}{\rho c_p}\frac{1}{r}\frac{\partial}{\partial r}\left(rq_r\right) \tag{3}$$

$$\frac{\partial C'}{\partial t'}+u\frac{\partial C'}{\partial x}+\frac{\partial C'}{\partial r}=\frac{D}{r}\frac{\partial}{\partial r}\left(r\frac{\partial C'}{\partial r}\right)-K_1C' \tag{4}$$

With boundary conditions,

$$\left.\begin{aligned} &t' \le 0 : u = 0, \quad v = 0, \quad T' = T'_\infty, \quad C' = C'_\infty \qquad \text{for all } x \ge 0 \text{ and } r \ge 0 \\ &t' > 0 : u = u_0 + u_0 Cos(\omega t), \; v = 0, \quad T' = T'_w, \quad C' = C'_w \qquad \text{at} \quad r = r_0 \\ &\qquad u = 0, \quad v = 0, \quad T' = T'_\infty, \quad C' = C'_\infty \qquad \text{at} \quad x = 0 \text{ and } r \ge r_0 \\ &\qquad u \to 0, \qquad T' \to T'_\infty, \quad C' \to C'_\infty \qquad \text{as} \quad r \to \infty \end{aligned}\right\} \tag{5}$$

By using Rosseland approximation from Gnaneswara Reddy (2009) the radiative heat flux q_r is

$$q_r = -\frac{4\sigma_s}{3K_e}\frac{\partial T'^4}{\partial r}$$

In order to linearized q_r , we expand T'^4 into Taylor series about T'_∞ and by neglecting the higher order terms takes is of the form

$$T'^4 \cong 4T'^3_\infty - 3T'^4_\infty$$

Then the equation (3) reduces to equation (5)

$$\frac{\partial T'}{\partial t'} + u\frac{\partial T'}{\partial x} + \frac{\partial T'}{\partial r} = \frac{\alpha}{r}\frac{\partial}{\partial r}\left(r\frac{\partial T'}{\partial r}\right) - \frac{16\sigma_s T'^3_\infty}{3K_e\rho c_p}\frac{1}{r}\frac{\partial}{\partial r}\left(r\frac{\partial T'}{\partial r}\right) \tag{6}$$

It is necessary to make the equations (1), (2), (4) and (6) with boundary conditions (5) dimensionless. For this intention we introduce the following dimensionless quantities

$$\begin{aligned} &U = \frac{u}{u_0},\ R = \frac{r}{r_0},\ \ X = \frac{x\upsilon}{u_0 r_0^2},\ V = \frac{vr_0}{\upsilon},\ t = \frac{t'\upsilon}{r_0^2}, T = \frac{T' - T'_\infty}{T'_w - T'_\infty} \\ &Gr = \frac{g\beta r_0^2 (T'_w - T'_\infty)}{\upsilon u_0},\ Gc = \frac{g\beta^* r_0^2 (C'_w - C'_\infty)}{\upsilon u_0}, C = \frac{C' - C'_\infty}{C'_w - C'_\infty} \\ &Pr = \frac{\upsilon}{\alpha},\ \ N = \frac{KK_e}{4\sigma_s T'^3_\infty},\ \ Sc = \frac{\upsilon}{D},\ \ K = K_r\frac{r_0^2}{\upsilon}, M = \sigma B_0^2\frac{r_0^2}{\rho\upsilon} \end{aligned} \tag{7}$$

If γ denotes the non-dimensional viscosity variation parameter then $\gamma = \lambda\,(T^*_w - T^*_\infty)$. By putting the non-dimensional quantities of (7) into the equations (1), (2), (4) and (6) along with (5), then we obtain the following no-dimensional equations (8) to (11) with boundary conditions (12)

$$\frac{\partial U}{\partial X} + \frac{\partial V}{\partial R} + \frac{V}{R} = 0 \tag{8}$$

$$\frac{\partial U}{\partial t} + U\frac{\partial U}{\partial X} + V\frac{\partial U}{\partial R} = GrT + GcC + (1+\gamma T)\left(\frac{\partial^2 U}{\partial R^2} + \frac{1}{R}\frac{\partial U}{\partial R}\right) + \gamma\frac{\partial U}{\partial R}\cdot\frac{\partial T}{\partial R} - MU \tag{9}$$

$$\frac{\partial T}{\partial t} + U\frac{\partial T}{\partial X} + V\frac{\partial T}{\partial R} = \frac{1}{Pr}\left(1 + \frac{4}{3N}\right)\frac{1}{R}\frac{\partial}{\partial R}\left(R\frac{\partial T}{\partial R}\right) \tag{10}$$

$$\frac{\partial C}{\partial t} + U\frac{\partial C}{\partial X} + V\frac{\partial C}{\partial R} = \frac{1}{Sc}\frac{1}{R}\frac{\partial}{\partial R}\left(R\frac{\partial C}{\partial R}\right) - KC \tag{11}$$

The corresponding boundary conditions in terms of non-dimensional variables are

$$\left.\begin{aligned} &t \le 0 : U = 0, \quad V = 0, \quad T = 0, \quad C = 0 \qquad \text{for all } X \ge 0 \text{ and } R \ge 0 \\ &t > 0 : U = 1 + cos(wt), V = 0, \; T = 1, C = 1 \text{ at } \quad R = 1 \\ &\qquad U = 0, \quad T = 0, \quad C = 0 \qquad \text{at} \quad X = 0 \quad \text{and } R \ge 1 \\ &\qquad U \to 0, \; T \to 0, \; C \to 0 \qquad \text{as} \quad R \to \infty \end{aligned}\right\} \tag{12}$$

Skin friction coefficient is presented by

$$\overline{C_f} = -\int_0^1 \left(\frac{\partial U}{\partial R}\right)_{R=1} dX \tag{13}$$

The rate of heat transfer rate is presented as

$$\overline{Nu} = -\int_0^1 \left(\frac{\partial T}{\partial R}\right)_{R=1} dX \tag{14}$$

3. NUMERICAL CALCULATION OF THE PROBLEM

An explicit finite difference method has been employed to solve the nonlinear partial differential equations (8)-(11) along with boundary condition (12). The finite difference equations for the equations (8)-(11) can be represented by the equations (15) to (18) respectively

$$\frac{U(i,j)-U(i-1,j)}{\Delta X}+\frac{V(i,j)-V(i-1,j)}{\Delta R}+\frac{V(i,j)}{1+(j-1)\Delta R}=0 \tag{15}$$

$$\frac{U'(i,j)-U(i,j)}{\Delta\tau}+U(i,j)\frac{U(i,j)-U(i-1,j)}{\Delta X}+V(i,j)\frac{U(i,j+1)-U(i,j)}{\Delta R}=$$
$$GrT(i,j)+GcC(i,j)-MU(i,j)-\left[1+\gamma T(i,j)\right]$$
$$\left[\frac{U(i,j+1)-2U(i,j)+U(i,j-1)}{(\Delta R)^2}+\frac{1}{\left[1+(j-1)\Delta R\right]}\frac{U(i,j+1)-U(i,j)}{\Delta R}\right] \tag{16}$$
$$+\gamma\frac{T(i,j+1)-T(i,j)}{\Delta R}\frac{U(i,j+1)-U(i,j)}{\Delta R}$$

$$\frac{T'(i,j)-T(i,j)}{\Delta\tau}+U(i,j)\frac{T(i,j)-T(i-1,j)}{\Delta X}+V(i,j)\frac{T(i,j)-T(i-1,j)}{\Delta R}$$
$$=\frac{1}{\Pr}\left[1+\frac{4}{3N}\right]\frac{1}{\left[1+(j-1)\Delta R\right]}\frac{T(i,j+1)-T(i,j)}{\Delta R}+\frac{1}{Pr}\left[1+\frac{4}{3N}\right]\left[\frac{T(i,j+1)-2T(i,j)+T(i,j-1)}{(\Delta R)^2}\right] \tag{17}$$

$$\frac{C'(i,j)-C(i,j)}{\Delta\tau}+U(i,j)\frac{C(i,j)-C(i-1,j)}{\Delta X}+V(i,j)\frac{C(i,j)-C(i-1,j)}{\Delta R}$$
$$=\frac{1}{Sc}\left[\frac{1}{\left[1+(j-1)\Delta R\right]}\frac{C(i,j+1)-C(i,j)}{\Delta R}+\frac{C(i,j+1)-2C(i,j)+C(i,j-1)}{(\Delta R)^2}\right]-KC(i,j) \tag{18}$$

To get the finite difference equations the region of the MHD flow is divided into the grids or meshes of lines parallel to *X* and *R* is taken normal to the axis of the oscillating cylinder. Here we consider that the height of the cylinder is $X_{max}=20.0$ i.e. *X* varies from 0 to 20 and regard $R_{max}=50.0$ as corresponding to $R\to\infty$ i.e. *R* varies from 0 to 50. In the above equations (11) to (14) the subscripts *i* and *j* designate the grid points along the *X* and *R* coordinates, respectively, where $X=i\Delta X$ and $R=1+(j-1)\Delta R$. $M=400$ and $N=300$ grid spacing in the *X* and *R* directions respectively. The level $\Delta X=0.067$, ΔR=0.25 and the time step $\Delta\tau=0.001$ have been fixed to analyze. In this case, spatial mesh sizes are reduced by 50% in one direction, and then in both directions, and the results are compared. It is regarded that, when the mesh size is decreased by 50% in both the direction, the results differ in the fourth decimal places. The computer takes too time to compute the numerical values, if the size of the time-step is small. From the boundary conditions given in equation (12), the values of velocity *U, V* and temperature *T* are known at time $\tau=0$; then the values of *U, V* and *T* at the next time step can be calculated. Generally, when the above variables are known at $\tau=n\Delta\tau$, the values of variables at $\tau=(n+1)\Delta\tau$ are calculated as follows. The finite difference equations (15) and (18) at every internal nodal point on a particular *i*-level constitute a rectangular system of equations. The temperature *T* is calculated from equation (17) at first at every *j* nodal point on a particular *i* -level at the (*n+1*) time step. By making the best use of these known values of *T*, in a similar way the velocity *U* at the *(1+n)* time step is calculated from equation (14). Thus the values of *T* and *U* are known at a particular *i* -level. Then the velocity *V* is calculated from equation (13) explicitly. This process is repeated for the consecutive *i* -levels. Thus the values of and *T* are known at all grid points in the rectangular region at the $(1+n)^{th}$ time step. This iterative procedure is repeated for several time steps until the steady state solution is reached.

4. RESULT AND DISCUSSION

In order to get the physical insight of the problem of the study, the velocity profile, temperature profile and concentration profile are express by assigning numerical values to different parameters encountered into the corresponding equations. The value of Schmidt number (*Sc*) are chosen for Hydrogen gas diffusing in electrically-conducting Air (*Sc*=0.20), Helium (*Sc*=0.30), Steam (*Sc*=0.60), Oxygen (*Sc*=0.66), NH_3 (*Sc*=0.78) and CO_2 at 25^0C (*Sc*=0.94). The value of Prandtl number (*Pr*) number

are chosen for air (*Pr*=0.71), water (*Pr*=7.0) and water at 4^0C (*Pr*=11.62). The Fig-2 depicts that when *Pr* and *Sc* changes then the velocity curves show different shapes for fixed values of *Gr, Gc, N, k, γ* and *M*. Due to the increasing value of *Pr* increases the viscosity of the fluid which tends to make the fluid tick. Which decrease the velocity of fluid. (Higher *Pr* leads to faster cooling of the plate like water *Pr*=7.0 in comparison to air *Pr*=0.71). Schmidt number decrease the molecular diffusivity. For this reason velocity curves downward due to increase the Schmidt number (*Sc*).It is also noticed from the Fig-3 that the decreasing value of *Pr* and *Sc* results to an increasing of velocity main flow. The Prandtl number physically relates the relative thickness of the hydrodynamic boundary layer and thermal boundary layer. The velocity increases with the decreases of the chemical reaction which indicates the Destructive chemical reaction indicates and the reverse is called constructive chemical reaction. The Fig-3 evinces that when the *K* changes then the velocity curves evince different shapes for fixed values of rest parameters. So our problem indicates the destructive chemical reaction. The increase values of magnetic parameter create a drug force known as Lorentz force that opposes the fluid motion. The Fig-4 indicates that when *γ* changes then the velocity, curves show different shapes for fixed values of other parameters. The velocity curve is in downward direction at the increasing values of *γ*. The thermal Grashof number signifies the ratio of the species buoyancy force to the hydrodynamic viscous force and the mass Grashof number signifies the relative effect of the buoyancy force to the viscous hydrodynamic force. When *Gr, Gc, M* changes then the velocity curves exhibit different shapes *is* uncovered by the Fig-5. As the velocity curves increases for increasing values of *Gr, Gc* where *M* Fixed and when *M* increases then the velocity curves decreases. The curves are in upward direction for the increasing value of *Gr* and *Gc*. The temperature profiles curves exhibit different shapes when *Sc* and *Pr* changes with fixed values of *Gr, Gc, N, k,γ* and *M* is shown by the Fig-6. The temperature profiles curve is in downward direction at the increasing values of *Sc* and *Pr.* Schmidt number decrease the molecular diffusivity. When the *Sc, Pr* and *K* changes then the concentration curves let on different shapes for fixed values rest parameters as shown in Fig-8 and Fig-9. By analyzing Fig-8 it is apparent that the curves are upward direction with the combination of decreasing values of *Sc* and *Pr*. Nusselt number (*Nu*) is increases with the decreases of *γ* which is uncovered by the Fig-9. Skin-friction increases with an increase of *γ* which is shown by the Fig-10. With the increases of viscosity variation parameter (*γ*) increases the values of stream which as shown in Fig-11 to Fig-13. The isotherm lines increases for the increasing values of Prandtl number (*Pr*) which is noted by the Fig-14 to Fig-16.

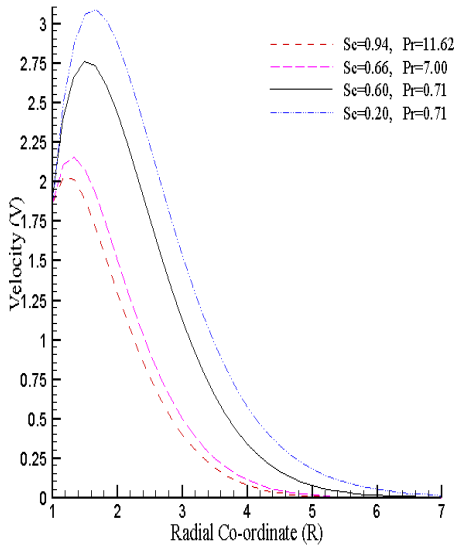

Fig-2:Velocity profiles for different values of *Sc* and *Pr* against *R.*

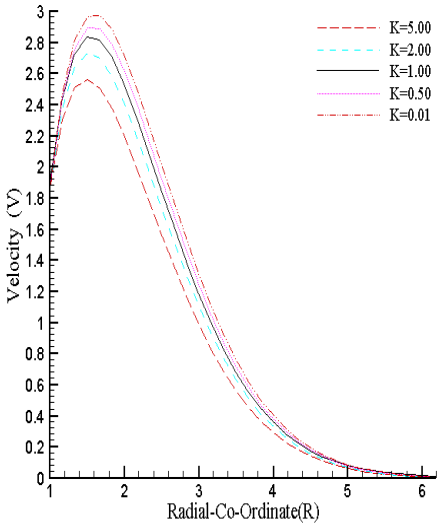

Fig-3:Velocity profiles for different values of *K* against *R.*

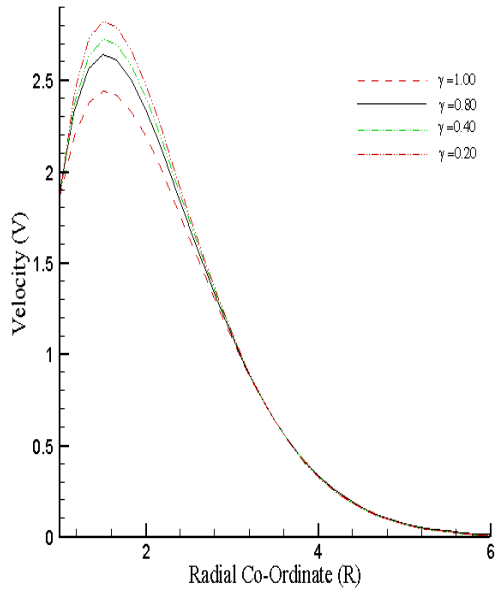

Fig-4: Velocity profiles for different values of *γ* against *R.*

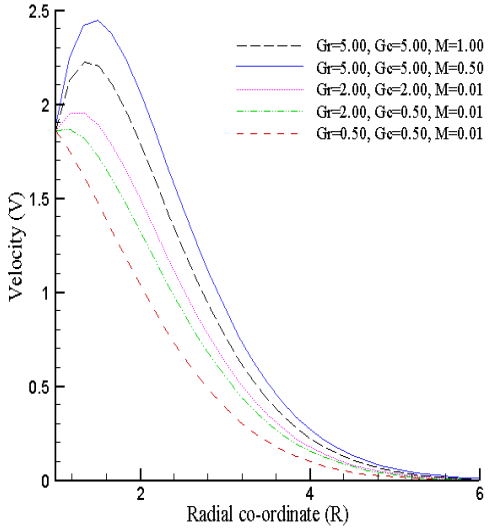

Fig-5: *Velocity profiles for different values of Gr, Gc and M against R.*

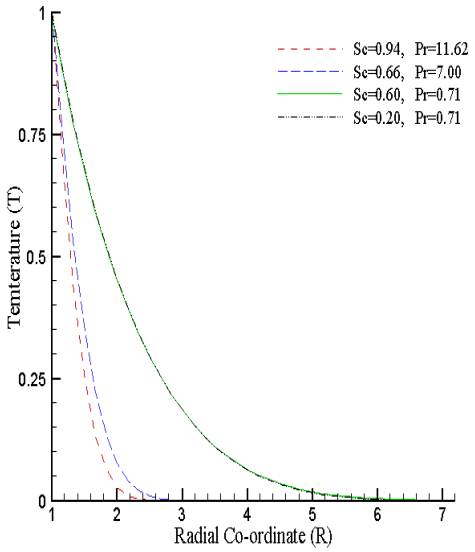

Fig-6: Temperature profiles for different values of *Sc* and *Pr* against *R*.

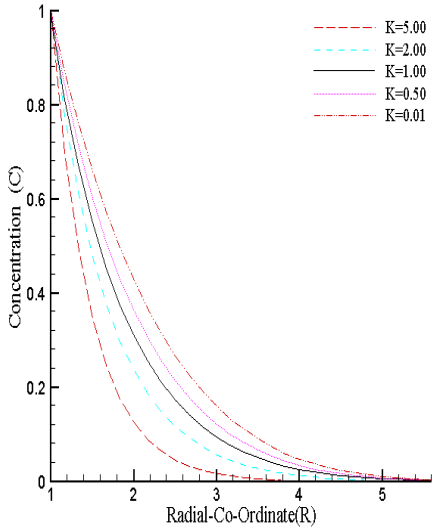

Fig-7: Concentration profiles for different values *K* against *R*.

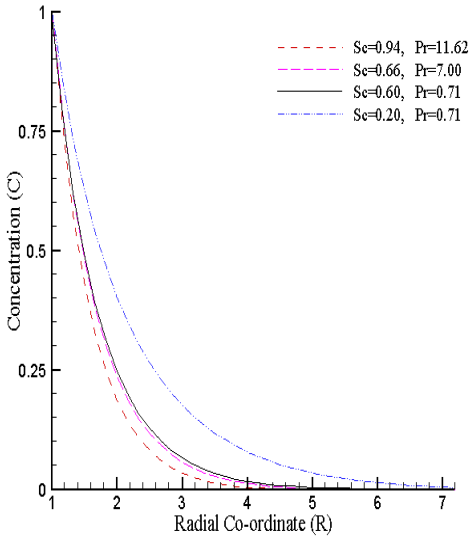

Fig-8: Concentration profiles for different values of *Sc* and *Pr* against *R*.

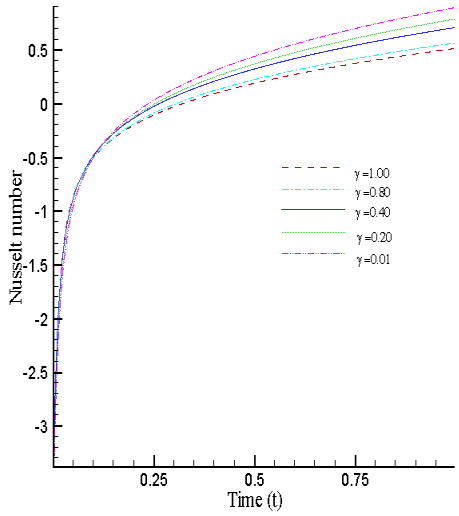

Fig-9: Nusselt number for different values of *γ* against *R*.

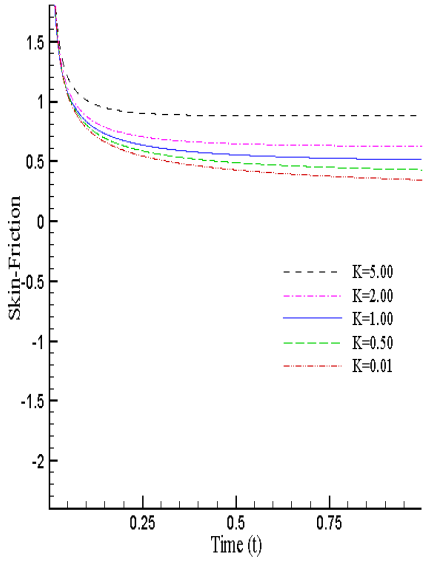

Fig-10: Skin-Friction for different values of *K* against *R*.

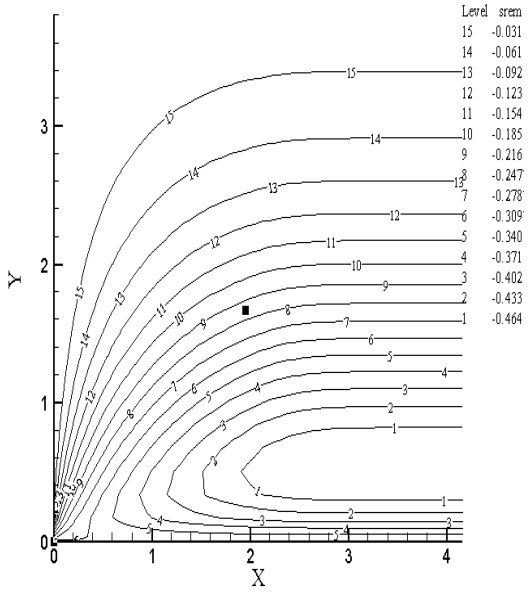

Fig-11: The streamlines with respect to *γ=-0.20* at *Pr=0.71*

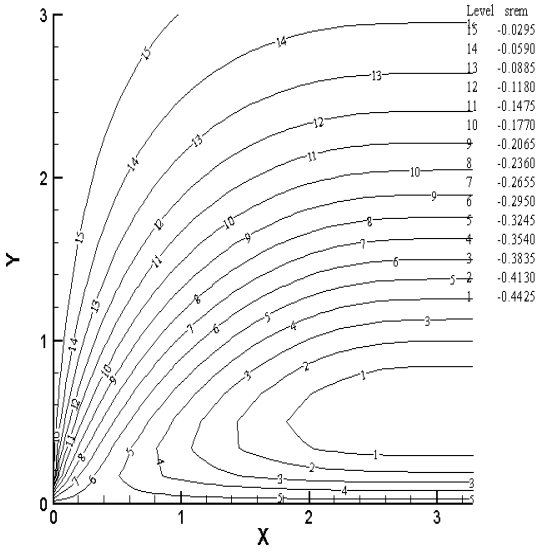

Fig-12: The streamlines with respect to γ=0.01at Pr=0.71

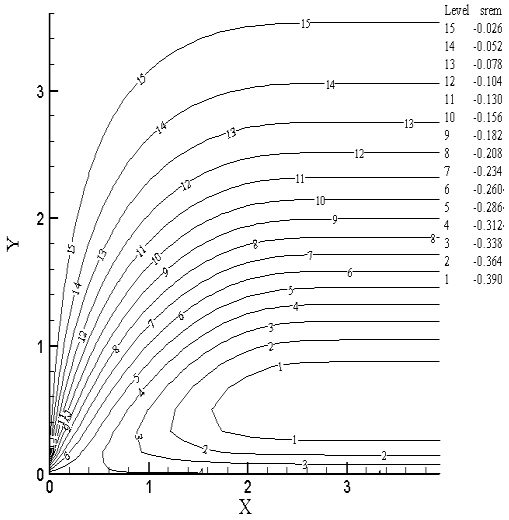

Fig-13: The streamlines with respect to *γ=0.80* at *Pr=0.71*

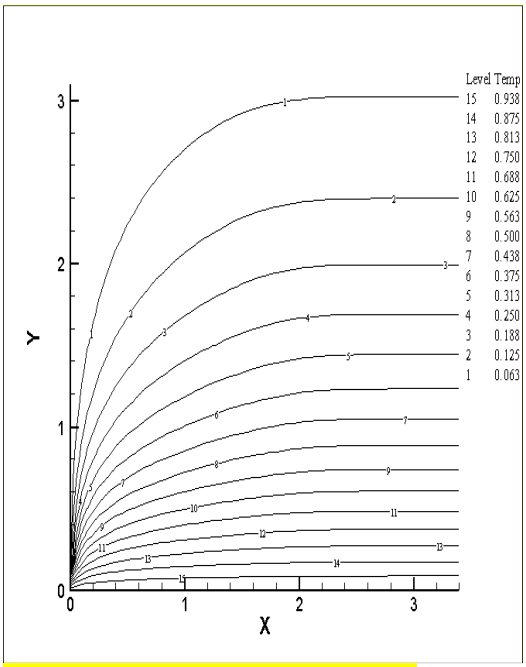

Fig-14: The isotherm lines at *Pr=0.71*

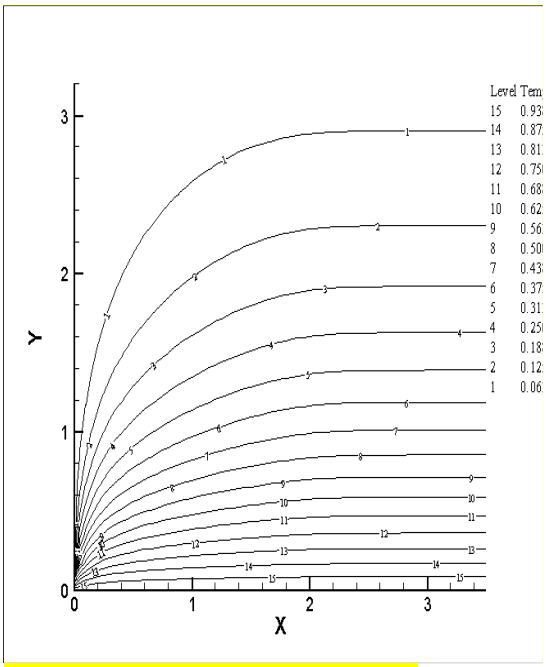

Fig-15: The isotherm lines at *Pr=0.78*

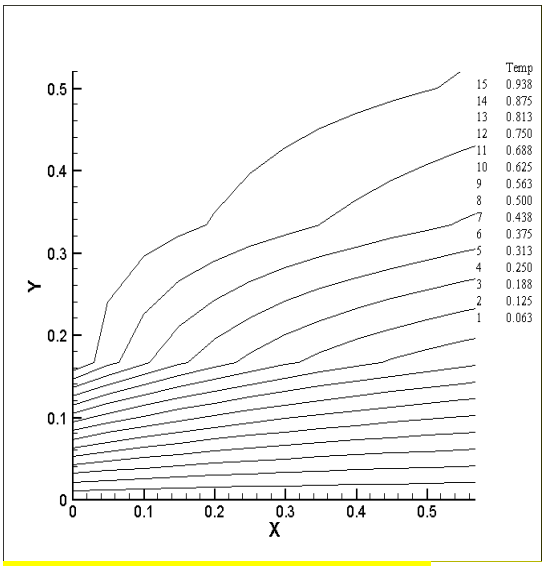

Fig-16: The isotherm lines at *Pr=11.62*

5. CONCLUTION

In the present research work, boundary layer equations become non-dimensional by using non-dimensional quantities. The non-dimensional boundary layer equations are nonlinear partial differential equations. These equations are solved by explicit finite difference method. Results are given graphically to display the variation of velocity, temperature, concentration, Nusselt number, Skin-friction, stream and Isotherm lines. The following conclusions are set out through the overall observations.

1) The velocity decreases with an increase of Scmidth number (*Sc*) and Prandtl number (*Pr)*.
2) With the decreasing of chemical reaction parameter (*K*), viscosity variation parameter (*γ*), result to increasing the velocity profiles.

3) For the decreasing values of Scmidth number (*Sc*) and Prandtl number (*Pr*) the temperature increases.
4) The concentration increases with the decreasing values of Scmidth number (*Sc*), Prandtl number (*Pr*) and chemical reaction parameter (*K*).
5) Skin friction increases with an increase of chemical reaction parameter (*K*).
6) The Nusselt number (*Nu*) is increases with the decreases of *γ*.

REFERENCES

Abd EL–Naby, M. A., El–Barbary, E. M. E. and Abdelazem, N. E. 2004. Finite difference solution of radiation effects on MHD unsteady free-convection flow on vertical porous plate, Applied. Mathematics, 151 (2): 327 – 346.

Alam and Rahman, M. S. 2006. Dufour and soret effects on mixed convection flow past a vertical porous flat plate with variable suction, Non-linear analysis of modelling and control, 11(1):03-12.

Beg, A., Bakier, A. Y. and Prasad, V. R. 2009. Numerical study of free convection magneto hydrodynamic heat and mass transfer from a stretching surface to a saturated porous medium with Soret and Dufour effects, Computational material science, 46: 57-65.

Das, S. S., Satapathy, A. J. and Panda, J. P. 2009. Mass transfer effects on MHD flow and heat transfer past a vertical porous plate through porous medium under oscillatory suction and heat source, International journal of heat and mass transfer, 52(25-26): 5962–5969.

Gnaneswara Reddy Machireddy. 2013. Chemically reactive species and radiation effects on MHD convective flow past a moving vertical cylinder, Ain shams engineering journal, 879–888.

Hossain, M. A., Mondal, R. K., Ahmed, R. and Ahmmed, S. F. 2015. A numerical study on unsteady natural convection flow with temperature dependent viscosity past an isothermal vertical cylinder, International journal of advanced research in engineering & management, 1(03): 91-98.

Mondal, R. K., Hossain, M. A., Ahmed. R. and Ahmmed. S. F. 2015. Free convection and mass transfer flow through a porous medium with variable temperature, American journal of engineering research: 01-07.

M. Gnaneswara Reddy, N. Bhaskar Reddy. 2009. Radiation and mass transfer effects on unsteady MHD free convection flow of an incompressible viscous fluid past a moving vertical cylinder. Theoret. Appl. Mech.3 (36): 239-260.

Popiel, C. O. 2008. Free convection heat transfer from vertical slender cylinder, Heat transfer engineering, 29(6): 521-536.

Rani, H. P. and Kim, C. Y. 2010. A numerical study on unsteady natural convection of air with variable viscosity over an isothermal vertical cylinder, Korean journal of chemical. Engineering, 27(3): 759-765.

Rajesh, V., Beg, A. and Sridev, C. 2016. Finite difference analysis of unsteady MHD free convective flow over moving semi-infinite vertical cylinder with chemical reaction and temperature oscillation effects, Journal of applied fluid mechanics, 9(1): 157-167.

Sharma B. R., Knowar Hemanta. 2015. MHD flow, heat and mass transfer due to auxiliary moving cylinder in presence of thermal diffusion, radiation and chemical reactions in a binary fluid mixture, International journal of computer applications,110(15).